



Modified SWAT to Forecast Water Availability in Mediterranean Mountainous Watersheds with Snowmelt Dominated Runoff

G. Harik^{1,2} · I. Alameddine² · M. Abou Najm³ · M. El-Fadel^{1,2} 

Received: 24 October 2022 / Accepted: 8 February 2023 / Published online: 11 March 2023
© The Author(s), under exclusive licence to Springer Nature B.V. 2023

Abstract

The assessment of the hydrological response to projected changes in climatic variables is imperative for water resources management, especially in watersheds where snowmelt represents a significant source of runoff. In this study, we modify the source code of the snow accumulation and melting algorithm of the Soil and Water Assessment Tool (SWAT) model to improve runoff simulations in snow dominated basins. A sinusoidal snowmelt function under the degree-day factor method was adopted with its parameters calibrated based on historical data. River flow simulations were compared to measured data under the modified and unmodified SWAT models. Model differences in future predictions of river flows (2032- RCP 4.5) were also assessed. The results showed that the modifications improved runoff simulations by better capturing flow dynamics as represented by daily flows and corresponding variability during the snowmelt period. The modified model increased the Nash–Sutcliffe Efficiency (from 0.64 to 0.79; 0.60 to 0.80; 0.70 to 0.75) and the coefficient of determination (from 48 to 67%, 48 to 69%, 58 to 70%) at three gauging stations. While both models predicted a decrease of water availability in the basin, future simulations with the modified snowmelt algorithm predicted that the drop in water availability as compared to baseline year (2008) will be less dramatic (24%) compared to predictions from the unmodified SWAT (31%). We argue that the proposed source code modifications to the snowmelt algorithm of SWAT provide better insights about future water availability in snow-dominated watersheds.

Keywords Snowmelt · SWAT · Water demand · Climate Change · Eastern Mediterranean

✉ M. El-Fadel
mutasem.elfadel@ku.ac.ae; mfadel@aub.edu.lb

¹ Department of Civil Infrastructure & Environmental Engineering, Khalifa University, Abu Dhabi, UAE

² Department of Civil & Environmental Engineering, American University of Beirut, Beirut, Lebanon

³ Department of Land, Air, and Water Resources, University of California, Davis, Davis, USA

1 Introduction

Most rivers have their headwater located at high elevations with snowmelt runoff invariably relied upon to meet water needs. In fact, mountains tend to receive a relatively large amount of precipitation, rain and snow, with snowmelt contributing significantly to annual runoff (Liu et al. 2020; Pepin et al. 2015). As such, the quantification of the hydrologic response to climate variations in agricultural mountainous catchments is critical for improved water resources management, particularly in areas experiencing chronic water shortages associated with population growth and exacerbated with climate change impacts. In this context, several types of rainfall–runoff models with different characteristics are commonly used to assess water flow and storage at the watershed scale (Bouslihim 2020; Pandey et al. 2020; Abbas et al. 2019) (Further details in Supplementary Material SM1).

In the context of watersheds with snow, snowmelt is a significant contributor to peak runoffs; yet few models support snowmelt simulations. These models rely on two main approaches namely, 1) the energy balance approach that is based on energy flux within the snowpack, which requires intensive data rarely available for mountainous regions; and 2) the degree day or the temperature index approach that has limited data requirements (Debele et al. 2010). Several studies compared the degree day factor method to the energy balance approach (Qi et al. 2017; Meng et al. 2015). Qi et al. (2017) reported a significant improvement in the accuracy of snowmelt prediction when switching from the degree day factor method (NSE 0.44) to the energy balance approach (NSE 0.74). While Meng et al. (2015) found that the relative error increased from 0.13 to 0.17 when switching from the degree day method to the energy balance approach. Other studies reported that the degree day approach can be as effective and accurate as the energy balance approach for small-scale watersheds (< 300 km²) (Haddeland et al. 2011; Guðmundsson et al. 2009).

The application of SWAT in snow-dominated watersheds outside the US have shown low to poor model skill because the snow module is based on empirical values for North America (Liu et al. 2020; Pandey et al. 2020). Few studies attempted to improve the SWAT snowmelt simulations by modifying the snow module or other input. Namely, Qi et al. (2016) proposed a new physically-based soil-temperature module in SWAT to address the intermediary role of snow cover. They introduced three new parameters to the original empirical soil-temperature module. While the integration was reported to improve the accuracy of snowmelt simulations, it did not modify the snowmelt processes. Qi et al. (2017) tried to modify the snowmelt module thereafter by modifying the energy balance snowmelt equations to improve the prediction of snowmelt in maritime regions. They reported improvement in the accuracy of predicting snowmelt as compared with the non-modified degree day factor process that is default in SWAT (NSE from 0.71 to 0.8, and R² from 0.75 to 0.84 for daily flows). Other studies attempted to explicitly modify SWAT's snowmelt module. Lui et al. (2020) and Duan et al. (2018) attempted to improve the snowmelt module, while relying on the degree day factor method. They reported that their modifications increased the accuracy of the snowmelt simulations slightly (NSE from 0.69 to 0.7 and from 0.71 to 0.75, R² from 0.76 to 0.78 and constant to 0.78, respectively).

SWAT has been applied in Mediterranean watersheds with limited snowmelt simulations. It has been used to estimate soil erosion (Bouslihim 2020) and to predict water availability (Saade et al. 2021; Martínez-Salvador & Conesa-García, 2020; Bouslihim et al. 2019). These studies indicated that the model had satisfactory precision in predicting flows. Saade et al. (2021) reported good model performance during calibration in the Nahr El Kalb watershed for two gauging stations in Lebanon using monthly flows. They reported NSEs ranging

between 0.57 and 0.78 and a percent bias (PBIAS) of 0.06% and -8.35%. Martínez-Salvador & Conesa-García (2020) reported good results when predicting monthly and yearly discharge and sediment loads in the Upper Argos River, in southeast Spain (NSE of 0.62 and 0.52; PBIAS of -20.6% and 10.65%, respectively). Similarly, Bouslihim et al. (2019) indicated that SWAT's performance was satisfactory when used to predict flows in the Mazer and El Himer (NSE=0.65). Nevertheless, all the above studies modeled discharge with limited snowmelt considerations. Yet, many mountainous Mediterranean watersheds receive large amounts of snow and require improvements to the snowmelt module in SWAT. Accordingly in this paper, we modified the SWAT snowmelt module using the degree day-factor method. We then conducted a parametric sensitivity analysis on the revised model and tested SWAT with and without the source code modification at a mountain watershed along the Eastern Mediterranean. The model was then used to predict potential water deficit and availability in the watershed as a function of climate change.

2 Methodology

2.1 Study Area

The study was conducted using data collected from the Damour watershed, a 290 km² mountainous watershed along the Eastern Mediterranean (Lebanon) (Fig. 1). The watershed's elevation ranges from 0 m at sea level (river mouth), to 1,980 m above sea level at the peak of the mountain (Khair et al. 2016). It encompasses several mountain ranges and plains lying within a river basin in addition to side streams, small and large tributaries with steep slopes, canyons, cliffs, and deep valleys reaching 700 m in some locations, along with high reliefs in many others (Khair et al. 2016). Nearly 50% of the watershed falls above 900 m elevation and ~25% above 1100 m, making these locations susceptible to snow and subsequent snowmelt that contributes significantly to Spring flows (Koeniger et al. 2017).

The area is characterized by a Mediterranean climate, with moderately warm and dry summers and moderately cold, windy, and wet winters with almost 80% to 90% of total precipitation occurring between November and March with scattered rainfall events beginning in October and ending in May (Khair et al. 2016). Temperatures decrease with elevation causing a shift from rain to snow mostly at elevations above 1000 m. Snow fall extends from November to April. The study area is dominated by a snow hydrologic regime influenced by accumulation and melting processes. Snowmelt occurring between March and May constitutes a significant source of fresh water for the coastal region with a Snow-Water Equivalent (SWE¹) that is moderately constant (~32 cm) in the winter and reaching its highest level (~114 cm) between mid-February (low elevation 1600 – 1980 m). Elevations lower than 1600 m encounter rain on snow events leading to quicker snowmelt (Fayad 2017).

2.2 Model Description and Setup

The SWAT model was used to simulate the long-term hydrological processes in the study area. SWAT is a physically based and a semi-distributed agro-hydrological model developed by the US Department of Agriculture (USDA) (Chiphang et al. 2020; Liu et al. 2020; Gong

¹ $SWE = HS\rho_s/\rho_w$; HS is the snow height in cm; ρ_s is the density of snow g/cm³; ρ_w is the density of water 1 g/cm³

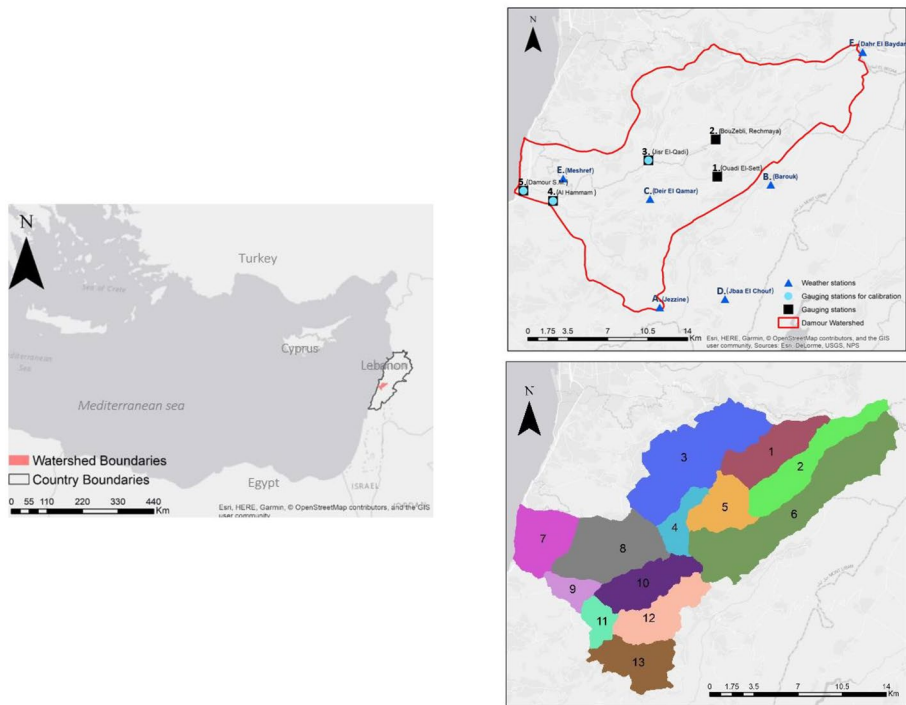


Fig. 1 Study area, sub-basins and gauging/weather stations within or near the study area watershed

et al. 2019; Monteiro et al. 2015; Narsimlu et al. 2015; Ravazzani et al. 2015; Arnold et al. 2012) (Further details in Supplementary Material SM2).

In this study, a 50 m × 50 m resolution DEM, spatially referenced to the WGS 1984 UTM-Zone 36N was used. The DEM was processed to generate several sub-basin properties such as channel slope, length and width. The DEM was also used to define flow direction and accumulation, create the stream network, choose the watershed outlets, delineate the watershed, and estimate sub-basin parameters (area, elevation, location, and slope). The 2017 land use—land cover (LULC) map of Lebanon was adopted (CNRS 2017) with reclassification to ensure that the LULCs types in the study area corresponded to those defined in SWAT. Similarly, the country's 2012 soil map (Darwish 2012) was used in the GIS layers representing the soil properties of the study area. The LULC and soil data were then analyzed with slope information to generate the hydrological response units (HRUs) (Gan et al. 2021; Neitsch et al. 2011). Monthly precipitation data were obtained from rainfall stations located in the watershed or within its immediate proximity (Further details in Supplementary Material SM2). Daily average, maximum and minimum temperature were gathered from the nearby Beirut Airport and a 6.5 °C decrease in temperature was used for every 1000 m change in elevation.

In the study area, terraces are common in agricultural lands with slopes exceeding 4%. Terracing was simulated in the model by adjusting the erosion and runoff parameters represented by the Universal Soil Loss Equation (USLE) parameters on land management practices, the curve number, and the slope length (Haan et al. 1994). The curve number was chosen according to the vegetation and soil type of the HRU. The maximum distance between

terraces was set at 10 m according to satellite images verified by field visits. The slope ranged between 2.3% and 73% with only one HRU associated with an extremely high mean slope (i.e. 73%) and is assigned to be barren in the LCLU map of 2017. Agricultural areas were mostly located near watercourses with soil types dominated with non-calcareous arenosol or clay anthrosols or gleysol corresponding to the Machias, Melrose and Lupton user soils in SWAT. Five sub-basins (1, 2, 3, 4, 6) have elevations above 900 m with a high likelihood to receive snowfall during the winter season (Further details in Supplementary Material SM2).

2.3 SWAT Snow Melting Module

The SWAT snowmelt module is separated into two parts, namely snowpack and snowmelt. Snowpack activation is based on the critical parameters that define the mean air temperature threshold that dictate the occurrence of snow. SFTMP (Snowfall temperature °C) represents the mean air temperature at which precipitation is equally likely to fall as rain or as snow/freezing rain. The precipitation would therefore be classified as snow when the mean daily air temperature is less than the snowfall temperature. Under such events, the liquid water equivalent of the snow precipitation would be added to the snowpack. This module relies on the snowpack mass balance:

$$SNO_i = SNO_{i-1} + R_{sfi} - E_{subi} - SNO_{mli} \tag{1}$$

where SNO_i is the snow equivalent at day i , SNO_{i-1} is the snow equivalent at day $i-1$, R_{sfi} is the snowfall equivalent of day i , E_{subi} is the evaporated snow equivalent of day i , and SNO_{mli} is the melted snow equivalent of day i .

The snowmelt module is activated when the snow cover conditions and the snowmelt temperature threshold is exceeded. In this study, the snowmelt module was based on the degree-day factor method. Under this method, a sinusoidal equation is used for snow-melting (Neitsch et al. 2011). This approach assumes that the potential snowmelt rate varies between a maximum and a minimum following a sinusoidal function based on the day of a year. The snowmelt runoff is derived from the snow cover condition and the temperature threshold of the snowmelt. The snow-melting temperature threshold is a manually set parameter. When the snow is completely melted, the resulting water would be the vertical depth of the water layer. The formula for snow melting calculation is presented in Eq. 4 (Neitsch et al. 2011).

$$T_{snow_i} = T_{snow_{i-1}}(1 - T_{IMP}) + T_{avi} T_{IMP} \tag{2}$$

$$SNO_{mli} = b_{mli} sno_{covi} ((T_{snow_i} + T_{maxi})/2 - SM_{TMP}) \tag{3}$$

$$b_{mli} = \frac{SMF_{MX} + SMF_{MN}}{2} + \frac{SMF_{MX} - SMF_{MN}}{2} \times \sin(2\pi \frac{i - 81}{365}) \tag{4}$$

where T_{snow_i} is the temperature of the snowpack at day i , T_{IMP} is the snow temperature lag factor, and T_{avi} is the mean air temperature at day i . SNO_{mli} is the amount of snowmelt at day i , b_{mli} is the melt factor for day i , sno_{covi} is the fraction of the HRU area covered by snow, SMF_{MX} is the snow melt factor for 21 June ($mm\ H_2O\ ^\circ C^{-1}\ d^{-1}$), SMF_{MN} is the snow melt factor for 21 December ($mm\ H_2O\ ^\circ C^{-1}\ d^{-1}$), T_{maxi} is the maximum air temperature at day i and SM_{TMP} is the snow melt base temperature (Arnold et al. 2012; Neitsch et al. 2011).

The SWE (Snow-Water Equivalent) is estimated using a linear function with the snowmelt factor method based on the mass balance for snow (Eq. 5) (Neitsch et al. 2011).

$$SWE_i = SWE_{i-1} + R_{day_i} - E_{sub_i} - SNO_{mli} \quad (5)$$

where SWE_i is the snow water equivalent at day i in mm H_2O , R_{day_i} is the amount of snowfall in day i in mm H_2O , E_{sub_i} is the snow sublimation at day i in mm H_2O and SNO_{mli} is the amount of snowmelt in day i in mm H_2O (Arnold et al. 2012; Neitsch et al. 2011).

2.4 Source Code Modification

The SWAT model was used for calibration and future prediction of water availability with and without modification of its source code to account for snowmelt and its impact on runoff simulations within the context of the study area. In the initial simulation, the default SWAT snowmelt module code was adopted with changes only made to calibrate the module to better represent the test area. The second simulation focused on modifying the snowmelt algorithm (Eq. 4) and its corresponding parameters² (Fig. 2).

2.4.1 Snow Parameters

The snow density is usually calculated from the snow-water equivalent and the depth of snow (i.e. snow density = SWE/depth). In this study, the snow density was measured on a daily basis. It ranged between 450 and 520 kg/m³ (Fayad 2017; DAHNT/NOVEC, 2016). The snowfall temperature of the area is usually ~2 °C and the snowmelt temperature is around 0.5 °C (Fayad 2017; DAHNT/NOVEC 2016). The snowpack lag temperature corresponds to the threshold of snow water content above which 100% of the surface is covered by snow. The fraction of the snow volume corresponding to 50% snow cover is usually represented by an exponential increase as a function of the snow water equivalent index (i.e. SWE/SWE_i, where SWE_i is the snow water equivalent with 100% of the area covered with snow). According to the available snow data in the study area, the best fit is for the 50% area coverage corresponding to a 0.3 ratio of snow depth at 100% coverage. Accordingly, the percentage of snow cover area is defined:

$$SNO_{covi} = \frac{SNO_i}{SNOCVMX} \left[\frac{SNO_i}{SNOCVMX} + \exp(cov_1 - cov_2 \frac{SNO_i}{SNOCVMX}) \right]^{-1} \quad (6)$$

where SNO_{covi} is the percentage of snow cover area at day i , $SNOCVMX$ is the equivalent to the minimum snow content when snow coverage is 100% and cov_1 and cov_2 are the shape coefficients of the curve. The influence of consecutive days (i and $i-1$) on the snowpack temperature is controlled by the lagging factor (Eq. 2). High elevations are accompanied by low atmospheric pressure and therefore high relative humidity that may cause a warmer feeling whereby the previous day can affect the snow-melting of the current day.

The regions of the study area covered with snow, returned a snow depth higher than 30 cm most of the time. When snow depth is higher than 30 cm (deep snow) the snow temperature is highly affected by air temperature. Due to the lack of temperature data for snow melt, an approximation of some available data showed that every 1 degree difference between the snow temperature at day i and its temperature at day $i-1$ corresponds to a 1.4 degree

² Snowfall temperature, snowmelt base temperature, maximum melt factor, minimum melt factor, snowpack lag temperature (i.e. influence of the snowpack temperature of the previous and current day), and the minimum snow water content.

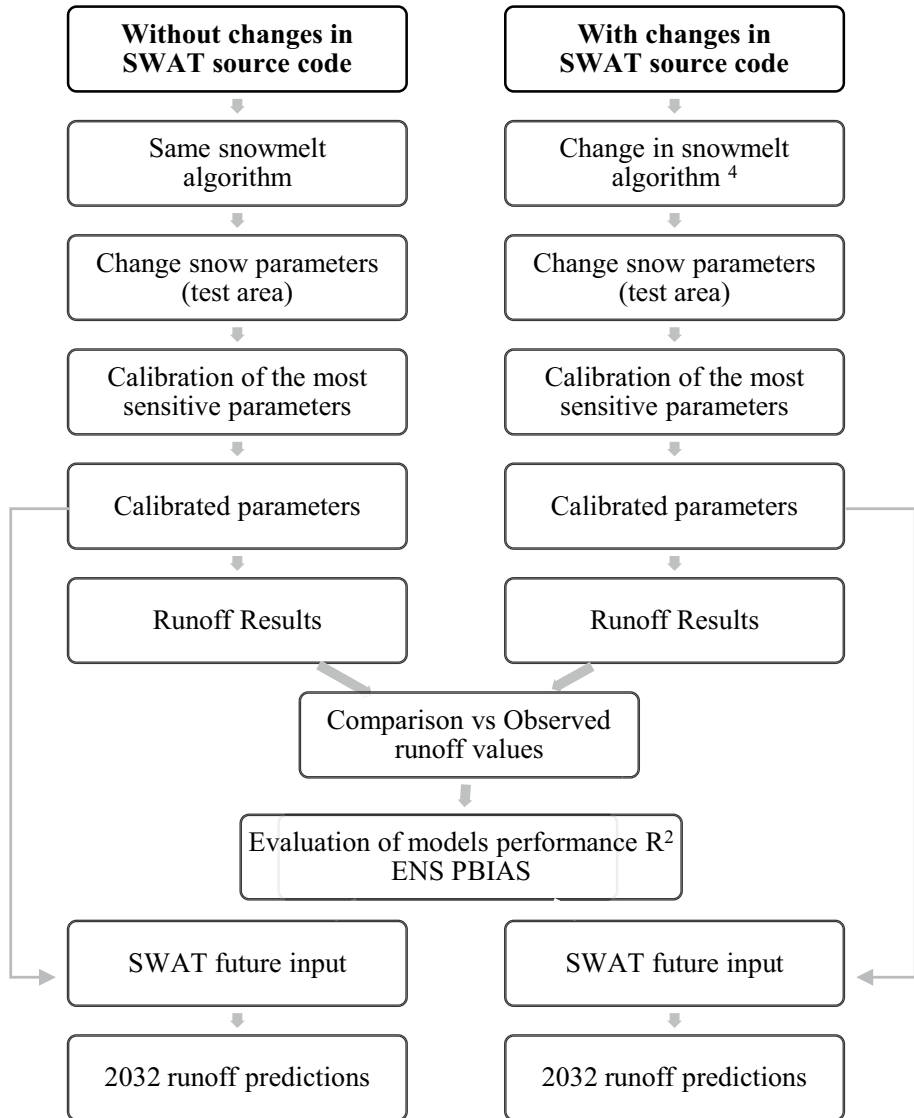


Fig. 2 Overall Modeling Framework

difference between the temperature of snow and air at day *i*. This assumption returned a 0.7 lag factor, higher than 0.5, and representing the pronounced impact of air temperature on the snow temperature compared to the impact of snow temperature of the previous day (Fayad 2017; DAHNT/NOVEC 2016; Arnold et al. 2012; Alexander, & Gong 2011). The minimum snow water content that corresponds to 100% snow cover (SNOCOV MX) was acquired from the combination of the historical snow data and satellite imagery. Satellite images were extracted from Landsat 7 for the period between 2015 and 2016 corresponding to the period

of snow data availability. The Normalized Difference Snow Index (NDSI)³ was calculated from the Landsat images based on bands 2 and 5 in Landsat 7 to identify the snow cover, while excluding regions with cloud cover. The NDSI is based on the ratio of (Green—SWIR) / (Green+SWIR), where Green refers to the reflectance in the green band of Landsat 7 and SWIR refers to the shortwave infrared reflectance. The NDSI ranges between 0.4 and 1 for snow (Riggs et al. 1994). Additionally, data from snow courses established by the government and that represent permanent stations to measure snow parameters were used. These stations included the Cedars (1800—2900 m asl), Mzar (1350—2350 m asl), and Laqlouq (1350-2350 m asl) stations, with a total of 649 snow course measurements. Each snow course was associated with snow depth, density and snow water content at each measurement date for each water year. For the dates with the lowest snow depth, Landsat TM images (Landsat 7) were analyzed to determine the date with 100% of the area covered with snow combined with a minimum snow depth. The dates with 100% of area covered with snow were accordingly delineated and the minimum corresponding snow water equivalent was chosen from the available snow data from the available snow stations. Therefore, the SNOCOMX was estimated at 10.2 cm.

2.4.2 Snowmelt Equation

In SWAT, the maximum and minimum melt factors are set according to the North American values and considered to be occurring on the 21st of June and 21st of December, respectively. As such, the source code was modified⁴ to account for the snow in terms of the snow melting. The snowmelt period was extended from early March to early June, with the minimum of snowmelt occurring at the beginning and end of the period and the maximum occurring around the middle of the period (April–May) (Fayad 2017; DAHNT/NOVEC 2016). Accordingly, the pre-imposed dates in the model were changed. The values of the degree-day factor (DDF in mm °C⁻¹ d⁻¹) were estimated based on the snow water equivalent and the air temperature (Eq. 7).

$$\text{DDF} = \frac{\text{SWE}}{\sum_1^N (\text{T}_B - \text{T}_t)} \quad (7)$$

where SWE is the snow water equivalent in mm, T_B is the average daily air measured temperature in °C/day and T_t is the average daily temperature threshold for snowmelt in °C/day. N is the number of days for all the snow to melt. The SWE was acquired from a data set at three nearby locations⁵ for the years 2015–2016. In the absence of characteristic snow data for this particular watershed, this data is the best representative estimate (Fayad 2017).

While a small decline in rainfall between 1967 and 2009 has been reported at a nearby catchment,⁶ a significant decrease in the snow residence time from 110 to 85 days (DAHNT/

³ The NDSI employs Landsat Thematic Mapper (TM) visible (0.56 /spl mu/m) and near-infrared (1.65 /spl mu/m) data. The snow algorithm uses the NDSI in combination with near-infrared reflectance to identify snow cover and discriminate snow from clouds.

⁴ The source code of SWAT 2012 revision 664 was accessed from <http://swat.tamu.edu/> and modified in Fortran 2013.

⁵ Permanent sites established by the government to measure snow parameters (<https://doi.org/10.5281/zenodo.583733>): Cedars (1800 – 2900 m asl), Mzar (1350 – 2350 m asl), and Laqlouq (1350 – 2350 m asl) at about 40 to 120 kms North of the study area with a total of 649 snow course measurements (30 different snow courses during snow season 2015 and 2016 with an average revisit time of 11.4 days)

⁶ Nahr Ibrahim about 50 kms north of the study area

NOVEC 2016) has been reported in the country, an evidence that climatic changes have resulted in higher melting rates. Snowmelt is not only driven by air temperature but mostly by the solar radiation that affects significantly the ablation of ice for its upper and lower parts and the lateral melting. In this context, the melting of snow occurs when the air temperature is above 0 °C and the longwave outgoing radiation falls above 316 W/m² (Hock 2003). The snow-melting period for all HRUs located at an elevation above 900 m was defined to extend from January 23 to April 26 with an SWE of 79.2 and 96.9 cm, respectively. The maximum snowmelt occurs around April 4 (Fayad 2017). By applying the DDF formula (Eq. 7) on the corresponding SWE and temperatures across all snowmelt periods, the minimum and maximum snow-melting factors were 2.2 and 2.8, respectively. The modification of the snowpack module in SWAT targets mainly the amount of snowmelt at day *i* formula (Eq. 4).

2.5 Model Calibration and Validation

In this study, the SUFI2 module of SWAT-CUP version 5.1.6 was used to examine the sensitivity, calibration, and validation of the model. This sequence starts with identifying the most sensitive parameters upon which to base the calibration (El Harraki et al. 2021; Praveen Kumar et al. 2019; Arnold et al. 2012). Fifteen parameters were chosen according to their occurrence among the main reported calibration parameters for variable flow rate (Ahmadisharaf et al. 2019; Abbaspour et al. 2018; Durães et al. 2011) (Further details in Supplementary Material SM3). A sensitivity ranking was then performed based on the t-stat or the ratio of the parameter coefficient by the standard error and the p-value that reflects the rejection of the hypothesis that an increase in the parameter value provides a significant increase in the variable response. Therefore, the most sensitive parameters were ranked according to the highest t-stat and lowest p-value.

The initial calibration and simulation used default values of SWAT snow parameters. The modified version of the source code was then run after changing the snow parameters. Both simulations were compared with field-flow measurements at three gauging stations with available monthly discharge measurements along the river⁷ (Fig. 1). Monthly discharge data between 2006 and 2009 were used for the initial calibration that consisted of 500 simulations until the objective function was reached (Nash–Sutcliffe efficiency coefficient > 0.6 for satisfactory results). The coefficients of determination (R^2) and Nash–Sutcliffe Efficiency (NSE) and the Percent Bias (PBIAS) were used to evaluate the model⁸ (Arnold et al. 2012). The parameters were then tested with available data that were not used for the calibration process, namely the years 2004 and 2005, to complete the validation process (El Harraki et al. 2021; Arnold et al. 2012).

⁷ 3. Jisr El-Qadi, 4. Al Hammam, 5. Damour Sea Mouth

⁸

0.75 < NSE ≤ 1.00	PBIAS ≤ ± 10%	0.75 < R ² ≤ 1.00	Very good
0.60 < NSE ≤ 0.75	± 10% < PBIAS ≤ ± 15%	0.60 < R ² ≤ 0.75	Good
0.36 < NSE ≤ 0.60	± 15% < PBIAS ≤ ± 25%	0.50 < R ² ≤ 0.60	Satisfactory
0.00 < NSE ≤ 0.36	± 25% < PBIAS ≤ ± 50%	0.25 < R ² ≤ 0.50 B	Bad
NSE ≤ 0.00	± 50% ≤ PBIAS	R ² ≤ 0.25	Inappropriate

NSE Nash-Sutcliffe Efficiency, PBIAS Percentage bias, R² Coefficient of determination

2.6 Water Availability Predictions

Future LULC data were obtained from an integrated Markov chain analysis with cellular automata approach using a GIS platform that was used for 2002 and 2017 to predict the linear trend of the watershed land cover change in 2032 (Further details in Supplementary Material SM4). Future Climate data were obtained from regional high resolution dynamical downscaling targeting extreme conditions of hottest and driest years for the study region (El-Samra et al. 2018) (Further details in Supplementary Material SM3).

3 Results and Discussion

3.1 Model Setup

The potential snowmelt rate of the study area varies between the minimum and the maximum occurring in January 23 and April 5 following a sinusoidal function based on the day of the year. The change of time in the predefined formula of the melt factor is 81 (Eq. 4), which corresponds to 81 days and calculated based on the minimum and maximum occurring in North America. In our study area, the minimum corresponds to the 23rd day of the year and the maximum to the 95th day. According to the principle that the snowmelt factor should be the maximum value of 1 on the 95th day, the sinusoidal function was modified to generate the maximum snowmelt at the 95th day and the minimum at the 23rd day (Eq. 4 modified to Eq. 8) and the source code was modified accordingly and re-compiled.

$$b_{mli} = \frac{SMF_{MX} + SMF_{MN}}{2} + \frac{SMF_{MX} - SMF_{MN}}{2} \times \sin\left(5\pi \frac{131 - i}{365}\right) \quad (8)$$

3.2 Model Calibration and Validation

The model sensitivity to parameters was ranked according to the p-value and t-stat. The most sensitive parameters were CH_K2, GWQMN, ALPHA_BF, SURLAG, REVAPMN, and GW_DELAY and chosen for p-values less than 0.3 and t-stats higher than 1.5 absolute. The calibration of those parameters resulted in the values ALPHA_BF=0.045, CH_K2=16.07, GW_DELAY=80.7, GWQMN=214.28, REVAPMN=89.29, SURLAG=1.18⁹ (Further details in Supplementary Material SM5).

The model was then run with and without the snowmelt modification with the respective calibrated parameter values. The runoff simulation results were close to observed flow data at the 3 gauging stations; yet the model systematically overestimated river flows (Fig. 3). At station number 3 (Jisr El Qadi), the NSE was 0.64 and 0.79 for the unmodified and modified code, which are considered good. The coefficient of determination (R^2) of the unmodified snowmelt module had a low value of 0.48, which increased significantly when modifying the source code reaching a good value of 0.67. The model bias (PBIAS) was 10% and 19%, which indicates that the model without the code modification tended to

⁹ ALPHA_BF: Baseline flow recession constant (days); CH_K2 Effective hydraulic conductivity of the channel (mm/h); GW_DELAY: Time interval for recharge of the aquifer (days); GWQMN: Water limit level in the shallow aquifer for the occurrence of base flow (mm); REVAPMN: Aquifer water depth for the occurrence of water rise to the unsaturated zone (mm); SURLAG: Delay time of direct surface runoff (days)

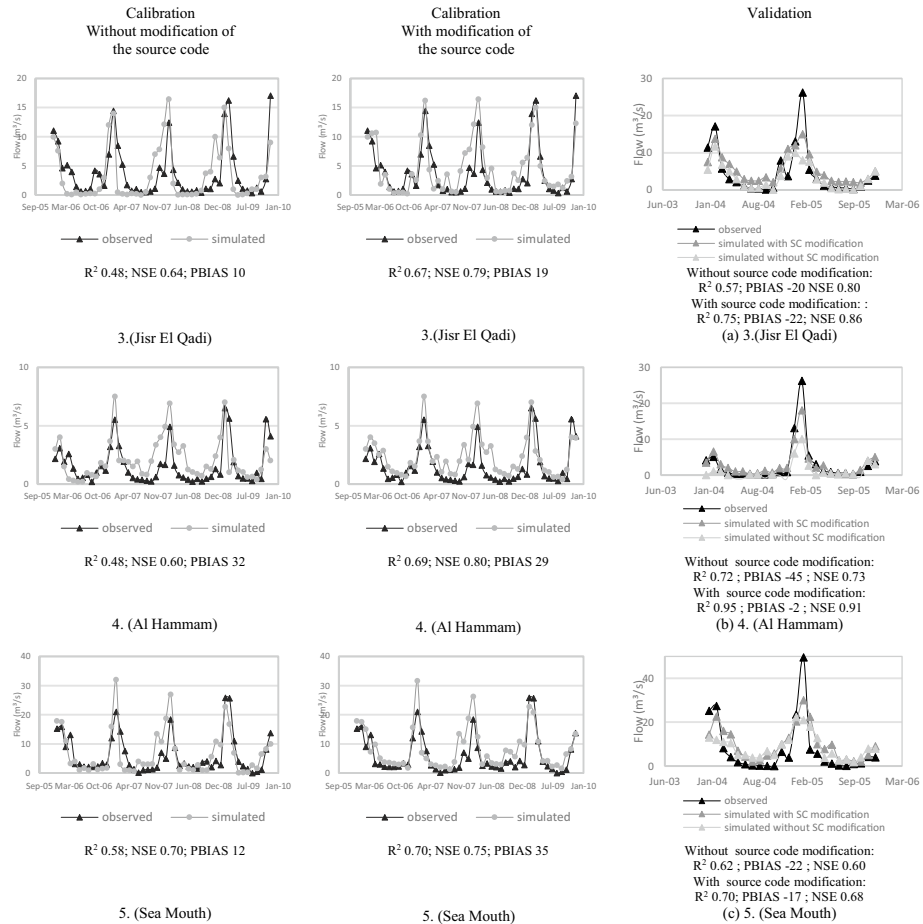


Fig. 3 Observed & simulated flows with & without source code modification (Calibration–Validation). * R2: Coefficient of determination; NSE: Nash–Sutcliffe Efficiency; PBIAS: Percentage of trend

overestimate the flows by 10%, and after the code modification, it overestimated the flows by 19%. At station number 4 (Al Hammam), the Nash–Sutcliffe Efficiency (NSE) was 0.6 and 0.8 (without and with source code modification, respectively) (Fig. 3). The coefficient of determination (R^2) of the non-modified model had a value of 0.48, which increased when modifying the source code to 0.69. The percentage of BIAS was 32% and 29% (without and with source code modification) decreasing the overestimation after source code modification. At station number 5 (sea mouth), the results were the most satisfactory. The NSE increased from 0.70 to 0.75 when modifying the source code. Similarly, the coefficient of determination (R^2) increased from 0.58 to 0.70. Meanwhile, the PBIAS indicated an overestimation of flows by 12 and 35% (Fig. 3).

While the simulation results before and after modifying the snowmelt module exhibited a good fit, when the modified code was used, the overall accuracy (NSE) increased compared to the original model. Additionally, some of the overall periodicity and peaks were captured adequately. The largest discrepancies between the two SWAT models (with and

without source code modification) were during the period between March and June, which is mostly affected by snowmelt. The original model predicted lower runoff during the snowmelt period. Moreover, the peak value of the simulated flows in the modified model occurs during the snowmelt period, indicating that the modification is effective (Fig. 3).

With regards to the validation period, overall the modified predictions were better than those generated by the original model, although the accuracy improvement was not large. The modified version of the model underestimated the flows at station 3 (Jisr El Qadi) by 22%, station 4 (Al Hammam) by 2%, and station 5 (Sea mouth) by 17%. Without source code modification, the model underestimated flows at stations 3 (Jisr El Qadi) by 20%, at station 4 (Al Hammam) by 45%, and at station 5 (Sea mouth) by 22%. The coefficient of determination (R^2) increased also between the unmodified and modified versions of the model for the three stations from 0.57 to 0.75 at station 3 (Jisr El Qadi), from 0.72 to 0.95 at station 4 (Al Hammam) and from 0.62 to 0.70 at station 5 (Sea mouth). Similarly, the NSE increased from 0.8 to 0.86 at station 3 (Jisr El Qadi), from 0.73 to 0.91 at station 4 (Al Hammam) and from 0.6 to 0.68 at station 5 (Sea mouth) (Fig. 3). Note that both formulations did not capture the extremely high discharge during February 2005, which was caused by one of the strongest storms recorded in the basin. The differences between both models are mainly highlighted for the snowmelt period between March and June. The results after the source code modification showed a significant increase in the flows during the validation of the model. These differences decreased from station 3 (Jisr El Qadi) to station 4 (Al Hammam) to station 5 (Sea mouth) from 119, to 48 to 36% (Fig. 3).

3.3 Water Availability Predictions

Future stream flows were simulated using the projected weather and LULC data. Considering 2008 as a reference of a dry and hot year, the predicted 2032 RCP4.5 precipitation decreased by 20% and 30% in the coastal and mountainous regions of the study area, respectively. Similarly, the 2032 maximum temperature increased by 2% along the coast and by 8% in the mountainous regions of the basin. The water yield represents the net amount of water contributing to stream flows including the surface runoff, lateral flow, and groundwater. The projected weather conditions of 2032 and LCLU with the use of the non-modified source code revealed a decrease in water yield for every month. A significant shortage of water flow all over the basin between March and October is expected. At sea mouth, after modifying the source code and with the projected weather conditions of 2032 and its LCLU, the results showed lower decreases in water availability for every month but with the same water shortage duration between March and October. The mean monthly water yield (Further details in Supplementary Material SM2) decreased by 24% compared to the baseline (i.e. 2008). The largest change still occurred in January reaching an average of 84% decrease in inflow in all sub-basins (Fig. 4). These results reflect the impact of the source code modification targeting the snow module, reflecting higher runoff and accordingly less water shortages.

The results of the 2032 projection without change in the snow module showed a decrease in the water availability in the first part of the year compared to the modified model. A significant change was also observed in the last month of the year where the water availability returned a higher value compared to the modified model. The future mean monthly water yield decreased by 31% compared to the baseline (i.e. 2008). These results highlight the differences between with and without source code modification in the snowmelt module in SWAT. A two-tailed t-test assessed between the two series of projected water yields (with and without source code modification) returned a p-value of 0.09 representing a significant

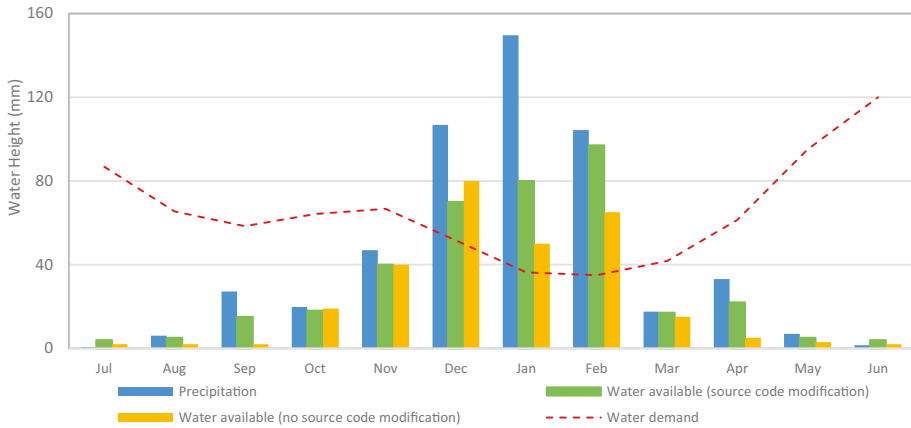


Fig. 4 Water deficit of 2032 at Station 5 (Sea Mouth)

difference between the modified source code model and the initial non-modified model at a 10% level. Therefore, an underestimation of runoff projections and water availability is expected without the source code modification in the context of snow simulations. This development highlights the importance of snowmelt simulations in mountainous catchments and the need to improve the simulation of such processes. SWAT can simulate hydrological processes including snow-generated runoff based on the snowpack and snowmelt modules. The snowpack module can be adjusted manually through the user interface, while the snowmelt module (usually applied based on site-specific empirical data) needs to be adjusted for better representation and improved simulations by targeting the refinement of the snow melting factor (b_{mli}) that resulted in greater water yield (runoff) from the snowmelt.

4 Conclusion

In mountainous watersheds snowmelt is often a significant source of runoff with a need for better hydrological characterization. In this study, the physically based hydrological model, SWAT was used with and without code modification of its snow module to improve runoff simulations. Proposed modifications were introduced because the model relies on empirical values for North America thus invariably requiring refinement to represent regions outside that region to improve runoff simulations. As such, the snowmelt algorithm was modified by targeting the improvement of the degree day factor method then SWAT was tested with and without this source code modification at a mountain watershed along the Eastern Mediterranean. The runoff simulation results were compared to field observed measurements then water availability and potential deficit were predicted. The source code modification improved runoff simulations with simulated river flows closer to observed measurements as reflected at three gauging stations in an increase in NSE and R^2 (0.64 to 0.79, 0.60 to 0.80, 0.70 to 0.75 & 48 to 67%, 48 to 69%, 58 to 70%). In addition, the modified snowmelt algorithm indicated an improvement in predicting future water yield whereby its corresponding decrease is expected to reach 24% in comparison to the 31% predicted without the source code modification. The source code modification to the snowmelt algorithm of SWAT appears to provide better insights about water deficit in snow-dominated watersheds that are increasingly under stress due to population growth and climate change.

Supplementary Information The online version contains supplementary material available at <https://doi.org/10.1007/s11269-023-03466-4>.

Author Contributions Ghinwa Harik: Conceptualization; Data curation; Formal analysis; Methodology; Calibration & Validation; Visualization; Writing - original draft. Ibrahim Alameddine: Conceptualization; Formal analysis; Methodology; Visualization; Writing - review & editing. Majdi Abou Najm: Formal analysis; Methodology; Visualization; Writing - review & editing. Mutasem El-Fadel: Conceptualization; Formal analysis; Methodology; Visualization; Writing - review & editing; Funding & Resource acquisition; Supervision & Project administration.

Funding This study was funded by the US Agency for International Development through the US Geological Survey, under the terms of Grant Number G17AC00079. The opinions expressed herein are those of the authors and do not necessarily reflect the views of the U.S. Agency for International Development or the U.S. Geological Survey (USGS).

Declarations

Competing Interests The authors have no relevant financial or non-financial interests to disclose.

References

- Abbas T, Hussain F, Nabi G, Boota MW, Wu RS (2019) Uncertainty evaluation of SWAT model for snowmelt runoff in a Himalayan watershed. *Terr Atmos Ocean Sci* 30(2):1–15
- Abbaspour KC, Vaghefi SA, Srinivasan R (2018) A guideline for successful calibration and uncertainty analysis for soil and water assessment: A review of papers from the 2016 international SWAT conference. July 25–29, Beijing, China
- Alexander P, Gong G (2011) Modeled surface air temperature response to snow depth variability. *J Geophys Res Atmos* 116(D14)
- Ahmadisharaf E, Camacho RA, Zhang HX, Hantush MM, Mohamoud YM (2019) Calibration and validation of watershed models and advances in uncertainty analysis in TMDL studies. *J Hydrol Eng* 24(7):03119001
- Arnold JG, Moriasi DN, Gassman PW, Abbaspour KC, White MJ, Srinivasan R, Santhi C, Harmel RD, Van Griensven A, Van Liew MW, Kannan N (2012) SWAT: Model use, calibration, and validation. *Trans ASABE* 55(4):1491–1508
- Bouslihim Y (2020) Hydrological and soil erosion modeling using SWAT model and Pedotransfert Functions: a case study of Settat-Ben Ahmed watersheds. Morocco (Doctoral dissertation, Université Hassan Ier Settat (Maroc))
- Bouslihim Y, Rochdi A, El Amrani P, Pazzi N (2019) Water balance estimation in Semi-arid Mediterranean Watersheds Using SWAT Model. In *Euro-Mediterranean Conference for Environmental Integration (1537–1543)*. Springer, Cham
- CNRS (2017) Land use/land cover map of Lebanon 2017. National Council for Scientific Research in Lebanon
- Chiphang N, Bandyopadhyay A, Bhadra A (2020) Assessing the Effects of Snowmelt Dynamics on Streamflow and Water Balance Components in an Eastern Himalayan River Basin Using SWAT Model. *Environ Model Assess* 25(6):861–883
- DAHNT/NOVEC (2016) Mise à jour des études et assistance technique pour la construction du barrage de Bisri. Detailed Design of Bisri Dam Project: Updated Hydrology Report. Council for Development and Reconstruction, Lebanon. Dar Al Handasah Taleb (DAHNT), NOVEC SA
- Darwish T (2012) Soil resources and soil database in Lebanon. CNRS-National Center for Remote Sensing. Extension of the European Soil Database Workshop
- Debele B, Srinivasan R, Gosain AK (2010) Comparison of process-based and temperature-index snowmelt modeling in SWAT. *Water Resour Manage* 24(6):1065–1088
- Duan Y, Liu T, Meng F, Luo M, Frankl A, De Maeyer P, Bao A, Kurban A, Feng X (2018) Inclusion of modified snow melting and flood processes in the SWAT model. *Water* 10(12):1715
- Durães MF, de Mello CR, Naghettini M (2011) Applicability of the SWAT model for hydrologic simulation in Paraopeba River Basin. *MG Cerne* 17(4):481–488

- El Harraki W, Ouazar D, Bouziane A, El Harraki I, Hasnaoui D (2021) Streamflow prediction upstream of a dam using SWAT and assessment of the impact of land use spatial resolution on model performance. *Environ Process* 8(3):1165–1186
- El-Samra R, Bou-Zeid E, El-Fadel M (2018) To what extent does high-resolution dynamical downscaling improve the representation of climatic extremes over an orographically complex terrain? *Theoret Appl Climatol* 134(1):265–282
- Fayad A (2017) Evaluation of the snow water resources in Mount Lebanon using observations and modelling (Doctoral dissertation). Hydrology. Université Paul Sabatier - Toulouse III, 2017. English. ffnNT:2017TOU30364ff.fttel-01755397v2f
- Gan R, Chen C, Tao J, Shi Y (2021) Hydrological Process Simulation of Sluice-Controlled Rivers in the Plains Area of China Based on an Improved SWAT Model. *Water Resour Manage* 35(6):1817–1835
- Gong X, Bian J, Wang Y, Jia Z, Wan H (2019) Evaluating and predicting the effects of land use changes on water quality using SWAT and CA–Markov models. *Water Resour Manage* 33(14):4923–4938
- Guðmundsson S, Björnsson H, Pálsson F, Haraldsson HH (2009) Comparison of energy balance and degree-day models of summer ablation on the Langjökull ice cap, SW-Iceland. *Jökull* 59:1–18
- Haan CT, Barfield BJ, Hayes JC (1994) Design hydrology and sedimentology for small catchments. Elsevier. First Edition - June 27, 1994. Copyright 1994 Elsevier Inc. ISBN 978-0-12-312340-4
- Haddeland I, Clark DB, Franssen W, Ludwig F, Voß F, Arnell NW, Bertrand N, Best M, Folwell S, Gerten D, Gomes S (2011) Multimodel estimate of the global terrestrial water balance: Setup and first results. *J Hydrometeorol* 12(5):869–884
- Hock R (2003) Temperature index melt modelling in mountain regions. *J Hydrol* 282(1–4):104–115
- Khair K, Kassem F, Amacha N (2016) Factors Affecting the Discharge Rate of the Streams-Case Study; Damour River Basin, Lebanon. *Journal of Geography, Environment and Earth Science International* 7(2):1–17
- Koeniger P, Margane A, Abi-Rizk J, Himmelsbach T (2017) Stable isotope-based mean catchment altitudes of springs in the Lebanon Mountains. *Hydrol Process* 31(21):3708–3718
- Liu Y, Cui G, Li H (2020) Optimization and application of snow melting modules in SWAT model for the alpine regions of Northern China. *Water* 12(3):636
- Martínez-Salvador A, Conesa-García C (2020) Suitability of the SWAT model for simulating water discharge and sediment load in a karst watershed of the semiarid Mediterranean basin. *Water Resour Manage* 34(2):785–802
- Meng XY, Yu DL, Liu ZH (2015) Energy balance-based SWAT model to simulate the mountain snowmelt and runoff - Taking the application in Juntanghu watershed (China) as an example. *J Mt Sci* 12(2):368–381
- Monteiro JAF, Strauch M, Srinivasan R, Abbaspour K, Gucker B (2015) Accuracy of grid precipitation data for Brazil: application in river discharge modelling of the Tocantins catchment. *Hydrol Process* 30(1):1419–1430
- Narsimlu B, Gosain AK, Chahar BR, Singh SK, Srivastava PK (2015) SWAT model calibration and uncertainty analysis for streamflow prediction in the Kunwari River Basin, India, using sequential uncertainty fitting. *Environ Process* 2(1):79–95
- Neitsch SL, Arnold JG, Kiniry JR, Williams JR (2011) Soil and water assessment tool theoretical documentation version 2009. Texas Water Resources Institute
- Pandey VP, Dhaubanjar S, Bharati L, Thapa BR (2020) Spatio-temporal distribution of water availability in Karnali-Mohana Basin, Western Nepal: Hydrological model development using multi-site calibration approach (Part-A). *J Hydrol Reg Stud* 29:100690
- Pepin N, Bradley RS, Diaz HF, Baraër M, Caceres EB, Forsythe N, Fowler H, Greenwood G, Hashmi MZ, Liu XD, Miller JR (2015) Elevation-dependent warming in mountain regions of the world. *Nat Clim Chang* 5(5):424–430
- Praveen Kumar C, Regulwar VD, Londhe SN, Jothiprakash V (2019) Determination of reservoir inflows from river basin using Soil and Water Assessment Tool (SWAT) and SWAT-CUP: A case study. In 11th World Congress on Water Resources and Environment: Managing Water Resources for a Sustainable Future-EWRA 2019. Proceedings
- Qi J, Li S, Jamieson R, Hebb D, Xing Z, Meng FR (2017) Modifying SWAT with an energy balance module to simulate snowmelt for maritime regions. *Environ Model Softw* 93:146–160
- Qi J, Li S, Li Q, Xing Z, Bourque CPA, Meng FR (2016) A new soil-temperature module for SWAT application in regions with seasonal snow cover. *J Hydrol* 538:863–877
- Ravazzani G, Barbero S, Salandin A, Senatore A, Mancini M (2015) An integrated hydrological model for assessing climate change impacts on water resources of the upper Po river basin. *Water Resour Manage* 29(4):1193–1215

- Riggs GA, Hall DK, Salomonson VV (1994) A snow index for the Landsat thematic mapper and moderate resolution imaging spectroradiometer. In Proceedings of IGARSS'94–1994 IEEE International Geoscience and Remote Sensing Symposium (Vol. 4, pp. 1942–1944). IEEE
- Saade J, Atieh M, Ghanimeh S, Golmohammadi G (2021) Modeling Impact of Climate Change on Surface Water Availability Using SWAT Model in a Semi-Arid Basin: Case of El Kalb River. *Lebanon Hydrology* 8(3):134

Publisher's Note Springer Nature remains neutral with regard to jurisdictional claims in published maps and institutional affiliations.

Springer Nature or its licensor (e.g. a society or other partner) holds exclusive rights to this article under a publishing agreement with the author(s) or other rightsholder(s); author self-archiving of the accepted manuscript version of this article is solely governed by the terms of such publishing agreement and applicable law.